UAV-BORNE GROUND PENETRATING RADAR FOR AVALANCHE FORECASTING

Bastien Dupuy[1]*, Martin Chatel[1,2], Arnt Grøver[1], Stéphane Garambois[3], Madeline Lee[1], Andrew Tobiesen[1], Halgeir Dhale[4], Sean Salazar[5], Regula Frauenfelder[5], Jordy Hendrikx[6,7], Tore Humstad[4]

[1] *SINTEF, Trondheim, Norway*
[2] *Ecole Polytechnique, Paris, France*
[3] *Université Grenoble-Alpes, CNRS, IRD, Univ. Savoie Mont Blanc, ISTerre, Grenoble, France*
[4] *Norwegian Public Roads Administration, Molde, Norway*
[5] *Norwegian Geotechnical Institute, Oslo, Norway*
[6] *The Arctic University of Norway UiT, Institute of Geosciences, Tromsø, Norway*
[7] *Antarctica New Zealand, Christchurch, New Zealand*

ABSTRACT: In the GEOSFAIR (Geohazard Survey from Air) innovation project for the Norwegian public sector, several UAV (Uncrewed Aerial Vehicles)-borne remote sensing payloads (LiDAR scanners; RGB, infrared, and multispectral cameras) were tested to gather information on the snow surface and its changes over time. For example, by comparing bare-earth and snow surface digital elevation models over time, it is possible to derive estimates of snow height and snow height changes. However, in addition to resolution limitations for snow height (which is dependent on the quality of baseline terrain models), none of these remote sensing methods can give information on the snow layering and snowpack properties. During the last three years, we tested UAV-borne GPR (Ground Penetrating Radar) sensors to get information on the subsurface of the snow, i.e., on snow height, snow layering and snow properties (snow density and liquid water content). Numerous field tests in real mountain conditions including mapping flat areas and BVLOS flights in avalanche starting zones enabled us to determine optimal operational flight guidelines. To optimize data quality, the GPR sensors should record data at an altitude less than 5 m above the snow surface, which requires altimeter and UAV terrain-following capabilities. Flying downslope at a speed up to 2-3 m/s and following the surface at 2-4 m have been shown to be the best compromise in terms of flight safety and data quality. In dry snowpacks, we use a shielded antenna with a 1 GHz central frequency, that penetrates up to 8-10 m of snow and can detect changes in layering down to a couple of centimeters. We show good correlations between snow pits and interpreted layers in the GPR data, especially when mapping melt-freeze crusts. By converting snow density to GPR wave velocity at a snow pit location, and by mapping snow surface and snow-ground interfaces, we are also able to derive high-resolution snow height maps which correlate well with snow height derived from LiDAR surveys with lower spatial resolution. UAV-borne GPR is a promising tool to provide remote snowpack information including high resolution snow height and snow layering and may be used to support local avalanche forecasting. Additional work is on-going to derive snow properties without the need for local snow pit information.

KEYWORDS: remote sensing, GPR, UAV, snow height, snow density

1. INTRODUCTION

UAV (Uncrewed Aerial Vehicle)-borne geophysical and remote sensing measurements are getting increasing focus for monitoring and characterization of cryosphere elements. Specifically, measurements of properties of the snow cover strongly benefit of the use of airborne remote sensing and geophysical data thanks to large coverage, efficiency, non-destructive data collection, and safety compared to ground measurements. GPR (Ground Penetrating Radar) is an especially relevant method for snow measurements as it relies on the propagation of electromagnetic (EM) waves that are sensitive to snow properties. In dry snow, the EM velocity is dependent on the snow density and in wet snow, on the snow density and the liquid water content.

The application of UAV-borne GPR for cryospheric applications (snow, ice and glaciers) is limited in the literature. For example, Jenssen et al. (2020) developed a custom-made stepped-frequency continuous wave system with directional antennas covering a frequency band between 0.7 and 4.5 GHz and show various field results from snowpack measurements with good data quality. Valence et al. (2022) take advantage of the high signal-to-noise ratio of impulse GPR with a 1.5 GHz shielded antenna to calculate snow properties from repetitive UAV-borne GPR and photogrammetry surveys. Using low frequency antennas, Ruols et al. (2023) demonstrate the potential of UAV-borne GPR to acquire high spatial density data on alpine glaciers, with considerations on flight speeds and flight altitude. Grathwohl et al. (2022) provide a review of current possibilities of UAV-borne GPR, not limited to snow and ice applications. Dupuy et al. (2024) provides an extensive set of tests to optimize UAV GPR data acquisition and processing with a special focus on snow height and snowpack layering.

In this paper, we give more detailed examples of what can be achieved by UAV-borne GPR, with a focus on snow height mapping and snowpack layering identification. We first describe the UAV platform and the radar sensor. In a second part, we describe the main data processing steps including an automatic picking algorithm that allows to calculate wave propagation time difference between snow surface and snow-ground interface automatically. Then, we show examples of a high-density survey for snow height mapping before focusing on internal layering in GPR data recorded along Beyond Visual Line of Sight (BVLOS) flights following steep mountain flanks.

All surveys are acquired in the Stryn municipality in Vestland county (western Norway). The site is located in the alpine valley of Grasdalen at 930-940 masl, near the Fonnbu avalanche research station of the Norwegian Geotechnical Institute (NGI).

2. UAV PLATFORM AND GPR SENSOR

The UAV GPR surveys are carried out using a DJI Matrice 300 RTK aircraft. The UAV is equipped with a terrain following system from SPH Engineering that uses a radar altimeter allowing to follow terrain at a given target altitude to optimize data quality and flight safety. The GPR system is a Radsys Zond Aero system with a 1 GHz shielded antenna. It has been shown (Dupuy et al., 2024) to have a good penetration depth in dry snow (up to 8-10 m) and an ability to detect thin layers (down to centimeter thickness if the contrast in density between the layers is large enough). Data is logged on an onboard computer (SPH Engineering Skyhub) and the GPR data is georeferenced with RTK-GPS data.

3. DATA ACQUISITION AND PROCESSING

In March 2024, we carried out an extended UAV GPR survey just south of the Fonnbu avalanche research station. The test site is a 140 x 40 m rectangle where high density GPR data was acquired, comprising 100 parallel profiles equally spaced. The crossline resolution is 0.5 m while the inline resolution is 0.04 m (50 traces per second at 2 m/s flight speed, resampled to 0.05 m after processing). Figure 1 shows the footprint of the GPR survey lines. In the background, the shaded relief map of the snow surface derived from a UAV LiDAR survey carried out on the same day is plotted.

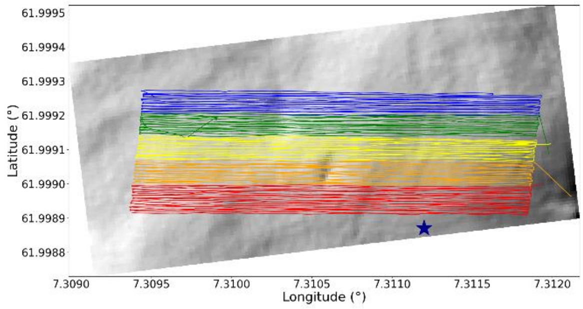

Figure 1: 100 GPR profiles covering a 140 x 40 m rectangle. The full surveys were carried out with five sets of UAV batteries corresponding to each set of colored lines. The background map is the shaded relief map visualization of the snow surface from UAV LiDAR survey. The blue star indicates the location of the snow pit where a density log was recorded.

4. DATA PROCESSING

GPR data processing follows an optimized custom workflow comprising several steps to enhance data quality, denoise data and preserve waveforms and amplitudes. The main steps are described in Dupuy et al. (2024) and include spatial resampling, time zero correction, background removal, bandpass and horizontal filtering, amplitude correction for spherical divergence and topography correction. As the dataset includes many profiles, the processing parameters are verified on one profile and applied to the other profiles automatically. In addition, automatic picking of the air-snow and snow-ground interfaces has been implemented using an amplitude threshold approach combined with spatial smoothing and correlation and outlier removals. Figure 2 shows an example of four different profiles of the full survey (Figure 1). The data shows large variability in snow height and demonstrates that the automatic picking method is satisfactory by allowing to derive automatically the two-way-travel times (TWT) between the snow surface and the snow-ground interface for all profiles.

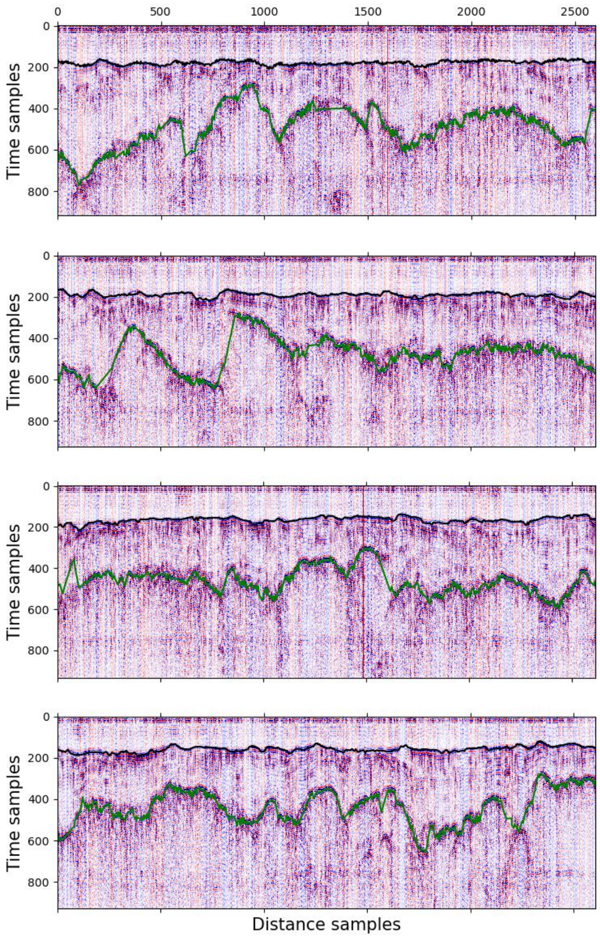

Figure 2: Four GPR profiles extracted from the survey described in Figure 1. The GPR data is processed (without topography correction) and automatic picking of the snow surface (black line) and the snow-ground interface (green line) is carried out.

5. SNOW HEIGHT MAPPING

After processing all GPR profiles and picking the snow surface and snow-ground interfaces, we know the TWT difference along all profiles. We recorded a density log profile where snow height is 270 cm (Frauenfelder, 2024). 10 layers with densities between 210 and 500 kg/m^3 and thicknesses between 6 and 20 cm were recorded. In a 2 cm thick melt-freeze crust at 200 cm height, and in the two base layers, density was not measured. For these layers, we extrapolate the velocity estimates by accounting for hand hardness changes (similarly to the approach of Kim and Jamieson, 2014, who estimate densities from hand hardness and grain types). Weighting by layer thicknesses, we obtain an average density that we convert to an average GPR wave velocity using Di Paolo et al. (2018) empirical relation. This relation links GPR wave velocity V_{GPR} with snow density ρ such as (c_0 being the EM wave velocity in the air): $V_{GPR} = \frac{c_0}{1+0.85\rho}$. We obtain an average GPR wave velocity of 22 +/- 2 cm/ns. The uncertainty on the effective velocity is estimated considering a 10 % error on the snow pit density measurements and a 2 cm layer thickness uncertainty (Proksch et al., 2016). Spatial variability of the snow densities and layer thicknesses is not considered.

Using this value, we convert the TWT differences of all profiles to snow heights and we carry out a spatial interpolation to calculate snow height maps. Figure 3 shows a comparison of LiDAR and GPR snow height maps using two different interpolation methods with the same parameters for both data types. The snow height derived from LiDAR data is calculated by subtracting the bare-earth surface model acquired by airborne laser scanning (ALS), with an average point density of 10 pts m^{-2} and raster cell resolution of 0.25 m x 0.25 m, from the UAV LiDAR data recorded over the snow surface. The UAV LiDAR data was acquired using a DJI Matrice 300 RTK aircraft and Zenmuse L1 LiDAR sensor. No ground control points were used; however, post-processing kinematic (PPK) corrections were applied to improve the accuracy of the flight trajectories and resulting snow surface model. The baseline bare ground model acquired by ALS has a lower surface point density and spatial resolution (0.25 m), which impacts the final resolution and reliability of the LiDAR snow height map. Thanks to GPR data density, the radial basis function (RBF) interpolated snow height from GPR data has a very high resolution and cannot be directly compared with the LiDAR data due to resolution difference. However, by using a kriging interpolation method, with the same parameters for both LiDAR and GPR data, we can compare the snow height maps. Figure 4 presents an estimation of the differences between the two results, with up to 60 % (1.2 m) of error at limited locations. Most of the differences are below 20 % (40 cm), however, which is correlated with the mean absolute error calculated for the entire survey and equal to 11 % (27 cm). Overall, the agreement between LiDAR and GPR snow heights is satisfactory but is affected by resolution limitations of the LiDAR model and by uncertainty in the snowpack effective GPR velocity which does not account for spatial variability. We also observe a systematic underestimation of the snow height in the GPR data, which is likely due to the automatic picking method and the complexity of the ground conditions (lots of boulders and creeks, see Figure 2). Other surveys (not displayed here) carried out on smoother bare earth terrain (e.g., grass slopes) shows lower differences in snow heights thanks to a more accurate picking of the snow-ground interface in GPR data.

The primary interest of snow height maps for avalanche forecasting is to estimate available snow volumes and consequently potential avalanche sizes. Using the average snow density from the snow pit density log in combination with the high-resolution snow height mapping derived from GPR data, we can – in a next step – derive snow water equivalent maps that can be useful for glacier mass balance, hydropower forecasts and flood monitoring.

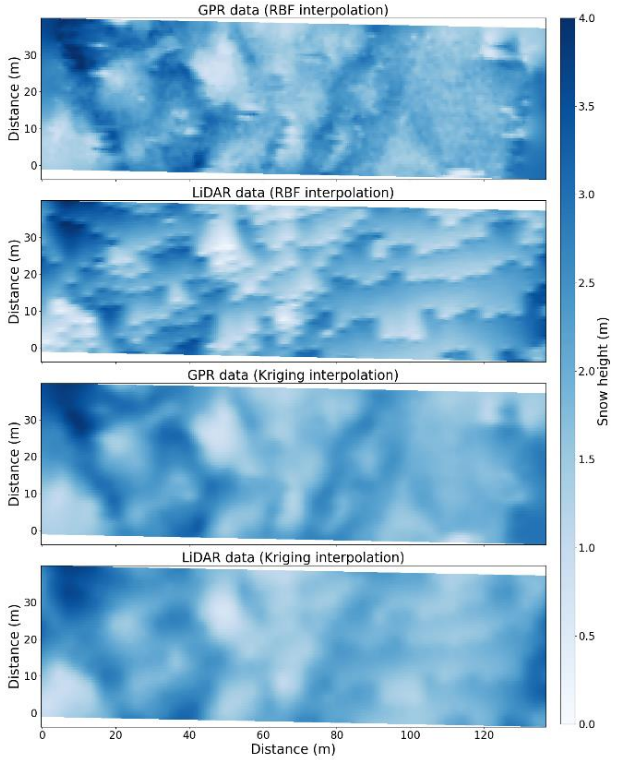

Figure 3: Snow height maps derived from UAV LiDAR and GPR surveys. From top to bottom: Snow height derived from GPR data using RBF interpolation method, snow height derived from LiDAR data re-interpolated using RBF interpolation, snow height from GPR data using kriging interpolation, snow height from LiDAR data using kriging interpolation.

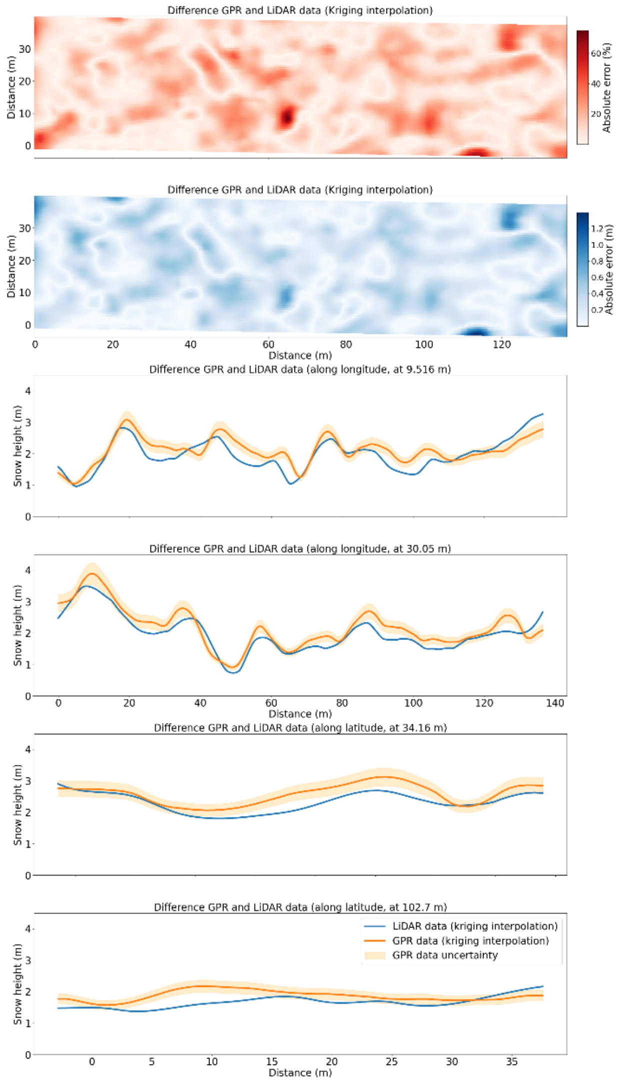

Figure 4: Differences and comparisons of snow heights calculated from LiDAR and GPR data and interpolated with the kriging method (Figure 3). From top to bottom: Absolute difference map between snow height from GPR and LiDAR data in percentage and in meters, cross sections of snow heights at different locations both inline (third and fourth rows) and crossline (fifth and sixth rows). The blue and orange lines stand for snow height derived from LiDAR and GPR data, respectively. The orange error bar around the orange line gives an estimation of the uncertainty of the GPR snow height related to the uncertainty in the GPR wave velocity.

6. SNOWPACK LAYERING

In addition to snow height mapping, we carried out extended BVLOS flights to record GPR data along the east flank of Sætreskarsfjellet mountain (1606 masl), west of Fonnbu research station. Flying downslope, we recorded a 945 m long profile with 288 m vertical elevation. For visual simplicity, we selected and interpreted three separate sections of the profile (Figure 5), from top to bottom of the slope (53, 72 and

60 m long respectively). Five snow pits were dug at different altitudes slightly north of the UAV GPR profile (Figure 5). We observe strong variations in estimated snow heights (estimated with an effective EM velocity of 21.21 cm/ns), with up to 4.8 m of snow in the top part and some sections with as little snow height as 0.8-1 m in the middle and bottom parts (Figure 5). We also observe some variations in the internal snowpack layering (number and location of the layers). The snow pits are located approximately 200 m north of the GPR line. We compare the GPR profiles with the snow pits closest in altitude even though we expect strong variations due to wind transport. Nevertheless, we find strong correlations between snow pits observations and GPR data, especially correlations in snow heights and layering. We observe several thin layers in the top part of the snowpack, while the bottom part is more compact and less layered.

7. CONCLUSIONS

We demonstrate that UAV-GPR data is relevant for high resolution snow height mapping. We could also show that UAV-GPR surveys allow for snow layer identification, thereby helping avalanche forecasters by providing data from large scale surveys in mountainous environments. Further validation and use of higher frequency antennas can help to improve the interpretation of the results. Additional work including Bayesian inversion and machine learning is on-going to derive snow properties (density, liquid water content) directly from the GPR data.

ACKNOWLEDGEMENTS

This study was funded by SINTEF strategic project GeoDrones and by the GEOSFAIR project, financed through the Research Council of Norway (grant no. 321035), the Norwegian Public Roads Administration, SINTEF and the Norwegian Geotechnical Institute. The Fonnbu avalanche research station receives support from the Norwegian Ministry of Oil and Energy through the project grants “R&D Snow avalanches 2020-2022 & 2023-2025” to NGI, administrated by the Norwegian Water Resources and Energy Directorate (NVE).

REFERENCES

Frauenfelder, R.: Regobs observation, https://regobs.no/registration/385805, 2024.

Di Paolo, F., Cosciotti, B., Lauro, S.E., Mattei, E. and Pettinelli E.: Dry snow permittivity evaluation from density: A critical review. In *2018 17th International Conference on Ground Penetrating Radar (GPR)*, pages 1–5, 2018

Dupuy, B., Grøver A., Garambois, S., Tobiesen, A., Lorand, P., Dahle, H., Salazar, S., Frauenfelder, R., Emmel, B., Einbu, A. and Humstad, T.: UAV-Borne GPR for Snow Mapping and Characterization. SSRN pre-print, 2023.

Grathwohl, A., Stelzig, M., Kanz, J., Fenske, P., Benedikter, A., Knill, C., Ullmann, I., Hajnsek, I., Moreira, A., Krieger, G., Vossiek, M., and Waldschmidt, C.: Taking a Look Beneath the Surface: Multicopter UAV-Based Ground-Penetrating Imaging Radars, IEEE Microwave Magazine, 23, 32–46, 2022.

Huber, E. and Hans, G.: RGPR — An open-source package to process and visualize GPR data, in: 2018 17th International Conference on Ground Penetrating Radar (GPR), pp. 1–4, 2018.

Jenssen, R. O. R., Eckerstorfer, M., and Jacobsen, S.: Drone-mounted ultrawideband radar for retrieval of snowpack properties, IEEE Transactions on Instrumentation and Measurement, 69, 221–230, 2020.

Kim D, Jamieson B.: Estimating the density of dry snow layers from hardness, and hardness from density. InProceedings of 2014 International Snow Science Workshop, Banff, Canada, 2014.

Looyenga H.: Dielectric constants of heterogeneous mixtures. Physica. 1;31(3):401-6, 1965.

Proksch, M. Rutter, N., Fierz, C., and Schneebeli, M.: Intercomparison of snow density measurements: bias, precision, and vertical resolution, The Cryosphere, 10, 371-384, 2016

Ruols, B., Baron, L., and Irving, J.: Development of a drone-based ground-penetrating radar system for efficient and safe 3D and 4D surveying of alpine glaciers, Journal of Glaciology, p. 1–12, 2023.

Valence, E., Baraer, M., Rosa, E., Barbecot, F., and Monty, C.: Drone-based ground-penetrating radar (GPR) application to snow hydrology, The Cryosphere, 16, 3843–3860, 2022.

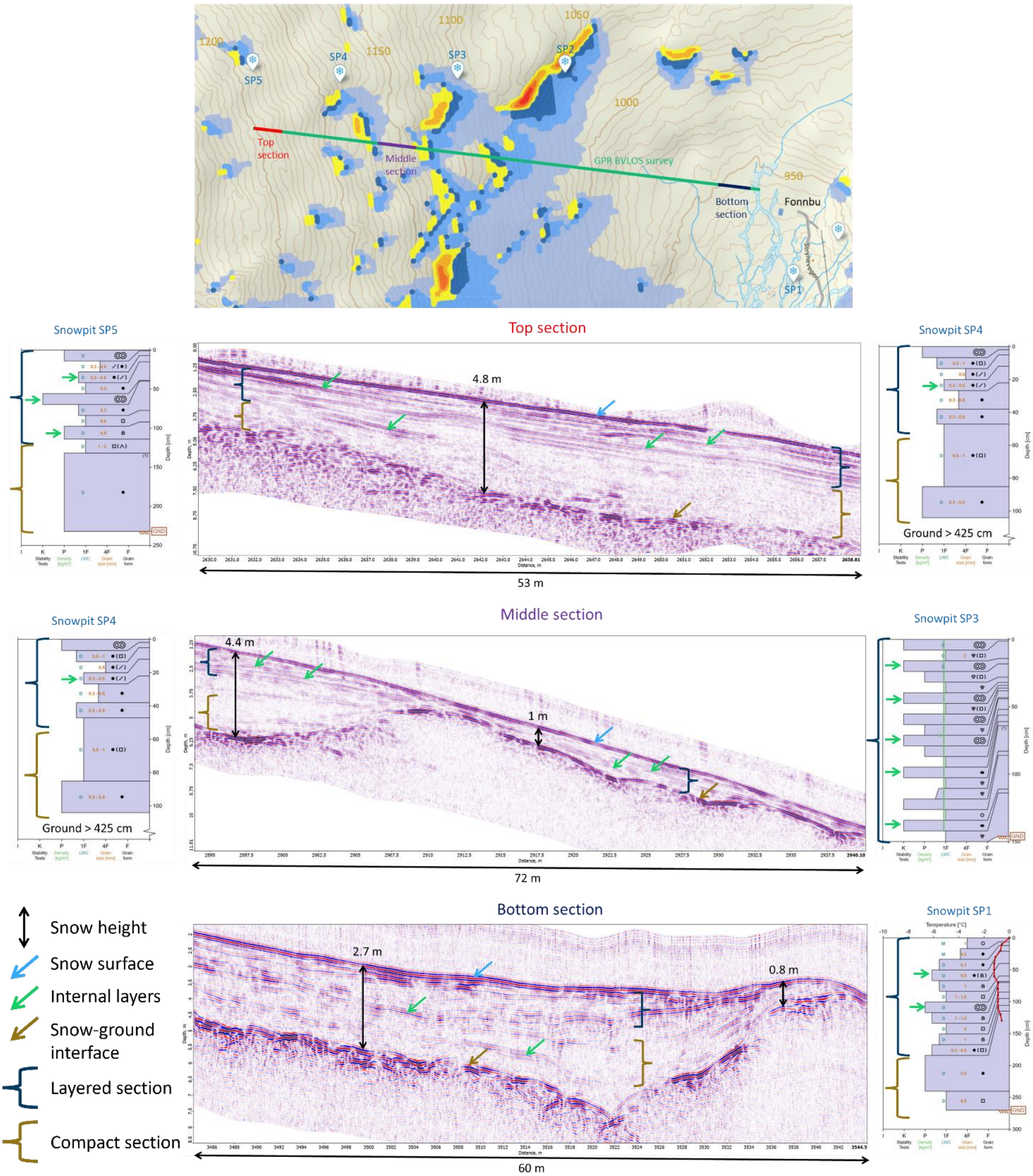

Figure 5: Example of a BVLOS UAV-GPR profile along a mountain slope. Top: map showing the location of the UAV-GPR profile (green line), the locations of snow pits SP1-5. The background map shows the contour lines with overlay of slope steepness (yellow, orange and red colors) and runout zones (blue colors). The full UAV-GPR survey (green line) is 945 m long and has a vertical elevation difference of 288 m. The start of the survey (i.e., top of the slope) begins at distance 2629 m (300 m elevation above take-off), and it ends at distance 3574 m (12 m elevation above take-off). For display purposes, we selected three representative sections (top section in red, middle section in purple and bottom section in dark blue). The three GPR profiles are plotted under the map (top to bottom: top, middle and bottom sections). The snow heights (black arrows) are estimated using an effective EM velocity of 21.21 cm/ns. The blue, brown and green arrows point to the snow surface, the snow-ground interface, and the internal snowpack layers, respectively. The blue and brown curly brackets indicate layered and non-layered (compact) parts of the snowpack. Correlation of GPR data with snowpack observations can be visually drawn by comparison with the snowpack observations plotted on both side.